

Constraining Jet/Disk Geometry and Radiative Processes in Stellar Black Holes XTE J1118+480 and GX 339–4

Dipankar Maitra^{1*}, Sera Markoff¹, Catherine Brocksopp², Michael Noble³,
Michael Nowak³ and Jörn Wilms⁴

¹ *Astronomical Institute “Anton Pannekoek”, University of Amsterdam, Kruislaan 403, 1098 SJ Amsterdam, The Netherlands*

² *Mullard Space Science Laboratory, University College London, Surrey RH5 6NT, UK*

³ *Kavli Institute for Astrophysics and Space Research, Massachusetts Institute of Technology, Cambridge, MA, USA*

⁴ *Dr. Karl Remeis-Observatory, University of Erlangen-Nuremberg, Sternwartstr. 7, 96049 Bamberg, Germany*

Accepted 2009 April 8. Received in original form 2008 June 9

ABSTRACT

We present results from modeling of quasi-simultaneous broad band (radio through X-ray) observations of the galactic stellar black hole (BH) transient X-ray binary (XRB) systems XTE J1118+480 and GX 339–4 using an irradiated disc + compact jet model. In addition to quantifying the physical properties of the jet, we have developed a new irradiated disc model which also constrains the geometry and temperature of the outer accretion disc by assuming a disc heated by viscous energy release and X-ray irradiation from the inner regions. For the source XTE J1118+480, which has better spectral coverage of the two in optical and near-IR (OIR) wavelengths, we show that the entire broad band continuum can be well described by an outflow-dominated model + an irradiated disc. The best-fit radius of the outer edge of the disc is consistent with the Roche lobe geometry of the system, and the temperature of the outer edge of the accretion disc is similar to those found for other XRBs. Irradiation of the disc by the jet is found to be negligible for this source. For GX 339–4, the entire continuum is well described by the jet-dominated model only, with no disc component required. For the two XRBs, which have very different physical and orbital parameters and were in different accretion states during the observations, the sizes of the jet base are similar and both seem to prefer a high fraction of non-thermal electrons in the acceleration/shock region and a magnetically dominated plasma in the jet. These results, along with recent similar results from modeling other galactic XRBs and AGNs, may suggest an inherent *unity in diversity* in the geometric and radiative properties of compact jets from accreting black holes.

Key words: black hole physics— radiation mechanisms: non-thermal and thermal— X-rays: binaries— stars: winds, outflows— accretion, accretion discs— X-rays: individual: (GX 339–4, XTE J1118+480)

1 INTRODUCTION

Soft X-ray transient (SXT) binary systems that occasionally go into episodes of high activity or *outbursts* are some of the best laboratories to study accretion flows near compact ($GM/R \sim c^2$) objects. Coordinated multi-wavelength campaigns have been carried out in recent years to observe SXTs simultaneously over a broad frequency range of nine decades or more from radio to X-rays (see, e.g., Fender 2006, for a review). These campaigns have provided extremely valuable insights about the accretion in/outflows and helped to constrain the theoretical models predicting accretion geometry and physical emission processes. Outbursts of SXTs are

usually explained in terms of a disc instability model (see, e.g., Lasota 2001, for a review), postulating a dramatic increase in mass accretion via an accretion disc towards the central compact object. The luminosity of a black hole transient (BHT) can vary by as much as eight orders of magnitude between quiescence and peak outburst, within timescales of weeks to months. Such systems are also ideal for studying the formation of jets, which are a by-product of accretion, yet poorly understood so far.

Matter spiralling into the gravitational potential well of the compact object forms an accretion disc, and radiates via dissipation of the accumulated gravitational potential energy. The observed UV and soft X-ray spectra of these sources, during epochs of high mass accretion rate, are well modeled by viscous dissipation from

* E-mail: D.Maitra@uva.nl

the inner regions of a geometrically thin, optically thick “Shakura–Sunyaev disc” (Shakura & Sunyaev 1973).

However in the OIR, the viscously dissipating disc model sometimes significantly underpredicts the observed spectral energy distribution (SED), and the excess is attributed to irradiation of the outer disc by the intense X-ray radiation from the inner region close to the compact object. This irradiation mechanism has been well explored theoretically (Cunningham 1976; Vrtilek et al. 1990; King et al. 1996; Dubus et al. 1999, 2001) and their effect observed in optical and near-IR wavelengths (e.g. Vrtilek et al. 1990; van Paradijs & McClintock 1994; McClintock et al. 1995; Hynes et al. 2002; Hynes 2005; Russell et al. 2006; Maitra & Bailyn 2008; Gierliński et al. 2009). The most prominent, observable effect of irradiation is to heat up the outer regions of the accretion disc to temperatures higher than what would be possible solely by viscous dissipation of a standard Shakura–Sunyaev disc. This leads to a deviation in the shape of the SED of the accretion disc (from that of a standard disc), creating a ‘bump’ in the optical through infra-red (OIR) wavelengths. As the quality of the OIR data improves, the deviation (i.e. the bump) from Shakura–Sunyaev spectrum becomes more and more apparent, and the need to incorporate irradiation in the model becomes important.

In Roche lobe overflowing BHTs where the accretor is 10 times or more heavier than the donor, X-ray irradiation of the donor is small. Furthermore irradiation causes the outer disc to flare, shielding most of the donor star from irradiation (Milgrom 1978). While most models assume an azimuthally symmetric accretion disc, warping of the accretion disc (see, e.g., Ogilvie & Dubus 2001, and references therein) can introduce additional uncertainties in shielding the donor from irradiation.

Not all the mass accreted inwards falls onto the compact object. Outflows, in the form of steady compact jets, or transient, ballistic ejecta are often seen in compact binary systems (see, e.g., Fender 2006, for a recent review). Steady, compact jets have been observed from an increasing number of compact binary systems when they are in an *X-ray hard state* (see below). The hallmark signature of such a jet is its flat to slightly inverted spectrum which, following the classic work by Blandford & Königl (1979), is usually attributed to a superposition of self-absorbed synchrotron emission from segments of a collimated jet. For stellar BHTs the flat spectrum of the jet is expected to extend from radio frequencies up to IR ($\sim 10^{13-14}$ Hz; Markoff et al. 2003), beyond which the jet synchrotron becomes optically thin (see, e.g., Corbel & Fender 2002). At X-ray frequencies, inverse Compton (IC) upscattering in the jet base of synchrotron as well as external photons from the accretion disc can become comparable and may even dominate the spectrum. As shown in Markoff et al. (2005), synchrotron and IC at the jet base can result in spectra very similar to those produced by compact Comptonizing coronal models (Poutanen 1998; Coppi 1999).

During the course of an outburst, the X-ray spectral and temporal features show an enormous amount of diversity. However extensive observations and their analyses over the past few decades have enabled the classification of spectral and temporal features into relatively few groups known as *X-ray states* (see, e.g., McClintock & Remillard 2006; Homan & Belloni 2005, for extensive definitions and review of X-ray states). In particular, two canonical states are often seen: a “soft” state characterized by strong thermal emission from the accretion disc and low variability in the light curve, and a “hard” state characterized by non-thermal power law emission, high variability and probably a collimated out-

flow. Besides these canonical states, a host of intermediate and extreme states with varying ratios of thermal and non-thermal radiation also are seen. Recent OIR observations (e.g. Maitra & Bailyn 2008; Russell et al. 2008) covering complete outbursts of many XRBs have shown that while irradiation usually plays a dominant role in the evolution of the OIR spectrum during the entire outbursting phase, the contribution from a non-thermal source, e.g. a jet, can become dominant when XRBs (most notably black holes) are in hard state. Thus any model which aims to understand disc-jet coupling must include irradiation.

We have developed a new spectral model which calculates continuum emission from an irradiated accretion disc, and in conjunction with a modified version of the compact jet model developed by Markoff et al. (2005), allows us to constrain the geometrical and radiative properties not only of the jet, but simultaneously those of the accretion disc. The thermal photons from the irradiated disc are also included in the photon field of the jet for Compton scattering, although due to Doppler redshifting in the jet frame, this external Compton emission is usually much smaller than the synchrotron self Compton (SSC). The new model is fully integrable with the standard spectral analysis software ISIS (Houck 2002) and parallelizable for using in large cluster computing environments (also see §3.3).

We have used this new model to analyze broad band quasi-simultaneous observations of two galactic BHT systems XTE J1118+480 and GX 339–4. Simultaneous or quasi-simultaneous observations of both sources, during hard X-ray state of their outbursts, have revealed broad band continuum emission ranging from radio to X-rays, strongly suggesting the presence of jets (Markoff et al. 2001, 2003; Homan et al. 2005; Markoff et al. 2005). By studying short time-scale variability in near-IR wavelengths from XTE J1118+480, Hynes et al. (2006) also suggested a non-thermal origin of the near-IR radiation, with a power law index typical of optically thin synchrotron emission from a jet.

The known physical properties of the two sources XTE J1118+480 and GX 339–4 have been briefly summarized in §2. Since analysis of multi-wavelength data requires careful calibration of data from various ground-based as well as space-borne instruments, we have also presented the data reduction and calibration procedures in §2. A brief outline of the model, with somewhat more emphasis on the newly introduced irradiated disc component, is given in §3, along with a description of the fitting procedure. The results of our broad band SED modeling suggest that despite the differences in size, mass, orbital parameters or accretion state, some of the fundamental physical parameters characterizing the geometrical and radiative properties of the jet are similar for both sources. This similarity may be a global property of jets formed near compact objects and is discussed in §4.

2 SOURCES, OBSERVATIONS & DATA REDUCTION

XTE J1118+480 and GX 339–4 are two prototype galactic BHTs with markedly different properties. Both binary systems contain high mass compact objects, $8.5 \pm 0.6M_{\odot}$ for XTE J1118+480 (Gelino et al. 2006) and $> 6 M_{\odot}$ for GX 339–4 (Muñoz-Darias et al. 2008), thus strongly suggesting for the compact objects to be black holes in both cases.

XTE J1118+480 lies $62^{\circ}.3$ north of galactic plane, in the halo. It has an orbital period of 4.04 hours (Gelino et al. 2006). The distance and interstellar column density to XTE J1118+480 are rea-

sonably well known from OIR photometry during quiescence to be 1.72 ± 0.1 kpc and $1.3 \times 10^{20} \text{ cm}^{-2}$ respectively (Gelino et al. 2006). We adopted a black hole mass of $8.5 M_{\odot}$ for this source. The orbital inclination of XTE J1118+480, as measured by Gelino et al. (2006) is 68 ± 2 degrees.

GX 339-4 lies near the galactic plane, only $4^{\circ}.3$ south of the galactic equator and has an orbital period of 42.14 hours (Hynes et al. 2003). We adopted a black hole mass of $7 M_{\odot}$ for GX 339-4 in this work. The secondary star in the GX 339-4 system has eluded detection so far, thus making estimates of masses, distance or line of sight extinction difficult. Here we have used a distance of 6 kpc and $N_{\text{H}} = 6 \times 10^{21} \text{ cm}^{-2}$ for GX 339-4, which are consistent with the limits given by Hynes et al. (2003, 2004) and Muñoz-Darias et al. (2008).

2.1 OIR and radio data

XTE J1118+480 went through an outburst during January-February 2005. A discussion of the OIR light curve morphology of the 2005 OIR outburst of XTE J1118+480 is presented by Zurita et al. (2006). It was noted by Zurita et al. (2006) that the 5-12 keV/ 3-5 keV hardness ratio from the *All Sky Monitor* (ASM; Levine et al. 1996) data onboard the *Rossi X-Ray Timing Explorer* (RXTE; Bradt et al. 1993) satellite suggested that the source was in an X-ray *hard* state during the entire outburst of 2005. For this source we used quasi-simultaneous optical (from the Liverpool telescope), near-IR (from UKIRT) and 15 GHz radio data (from the Ryle telescope). The full set of multi-wavelength observations obtained during this outburst of XTE J1118+480 will be presented in Brocksopp et al. (in prep).

XTE J1118+480 went through an outburst in 2000 as well. During this outburst the source was extensively observed by many ground based telescopes as well as space-borne missions (see e.g. Hynes et al. 2000; McClintock et al. 2001; Frontera et al. 2001; Chaty et al. 2003). In particular, the source was observed quasi-simultaneously around 2000 April 18th using the Ryle radio telescope, UKIRT, HST, EUVE, Chandra and RXTE giving an unprecedented broadband spectral coverage. This excellent data set has been used in several works (e.g. Markoff et al. 2001; Esin et al. 2001; Yuan et al. 2005) to infer properties of the source. We revisit this data set to constrain the geometry and radiative properties of both the jet and the disc using our new disc+jet model.

We used the OIR and radio SED of GX 339-4 reported by Homan et al. (2005), which were obtained during a multi-wavelength campaign to observe its outburst of 2002. For all data sets we used the photometric OIR magnitudes and de-reddened them using the interstellar extinction law of Cardelli et al. (1989). In the absence of definitive measurement of the ratio of total to selective extinction ($R_V [= A_V/E(B-V)]$) in the direction of either of the sources, we have taken $R_V = 3.1$, the widely used value measured by Rieke & Lebofsky (1985) towards the galactic center, and standardly used for these sources. Thus it must be kept in mind that if the “true” value of R_V is significantly different from 3.1 (given neither of the sources are very close to the galactic center), it might introduce additional uncertainty in reddening correction.

2.2 X-ray data

For both sources, we used data from the *Proportional Counter Array* (PCA; Jahoda et al. 2006) and the *High Energy X-Ray Timing Experiment* (HEXTE; Rothschild et al. 1998) onboard the

RXTE satellite. The X-ray data were downloaded from the NASA HEASARC’s public archive¹ and reduced using an in-house script following the standard reduction procedures outlined in *RXTE cook book*² using HEASOFT software (v6.1.2 Arnaud 1996). To avoid any terrestrial contamination, we considered data only for elevation angles of 10° or higher. Also any data with pointing offset more than $0^{\circ}.02$, or within 30 minutes of SAA passage, or trapped electron contamination ratio more than 0.1 were rejected. Since both the sources were bright (PCU2 count rate > 40 counts/s/PCU), the model *pca.bkgd.cmbrightvle.eMv20051128.mdl* was used for background subtraction. Data from all the layers of the active PCUs during the observations were extracted to create the spectra. Systematic uncertainty of 0.5% was added in quadrature to the PCA data to account for uncertainties in the calibration. For the HEXTE instrument, data from both clusters were added. Both PCA and HEXTE data were binned to achieve a minimum S/N of 4.5. For the PCA we used the energy range of 3-22 keV and for HEXTE 20-200 keV. The normalization of the OIR and radio data was tied to that of PCA. HEXTE normalization was allowed to vary.

3 MODEL, ANALYSIS AND RESULTS

The continuum jet model used in this work is based on Markoff et al. (2005), (henceforth referred to as the *agnjet* model). Given the importance of irradiation in the observed spectra of XRBs, we have modified the model to include additional physics (see §3.2 for details) that allow us to calculate the effect of irradiation on the outer disc due to high energy photons from (1) the jet, and (2) the inner regions close to the compact object, impinging on the disc. We also compute inverse Compton scattering of thermal disc photons by the electrons in the jet plasma, although their effect on the total spectrum is negligible, except near the jet base, due to Doppler redshifting of the disc photons in the jet frame.

3.1 Jet parameters

The details of the physics of the jet model as well as a full description of its main input parameters is given in the appendix of Markoff et al. (2005). Therefore we only give a brief summary here, and outline the modifications made to the Markoff et al. (2005) model:

The main parameters that determine the properties of the jet are the input jet power (N_j), electron temperature of the relativistic thermal plasma entering at the jet base (T_e), the ratio of magnetic to particle energy density (a.k.a. the equipartition factor k), physical dimensions of the jet base (assumed to be cylindrical with radius r_0 and height h_0), and the location of the point on the jet (z_{acc}) beyond which the a significant fraction of the leptons are accelerated to a power law energy distribution. N_j , parameterized in terms of the Eddington luminosity, determines the power initially input into the particles and magnetic field at the base of the jets. In the absence of a full understanding of the mechanism for energizing the jets, N_j plays a similar role to the compactness parameter in thermal Comptonization models (Coppi 1999). A typical value of the number density of leptons (n) at the base of the jet (derived from fits) is $n = N_j L_{\text{Edd}} / (4\gamma_s \beta_s m_p c^3 \pi r_0^2) \sim 10^{14-15} \text{ cm}^{-3}$. Here L_{Edd} is the Eddington luminosity of the source, $\beta_s \sim 0.4$ is the sound speed at

¹ <http://heasarc.gsfc.nasa.gov/docs/archive.html>

² http://heasarc.nasa.gov/docs/xte/recipes/cook_book.html

the base (see below), $\gamma_s = (1 - \beta_s)^{-1/2}$, m_p is the proton rest mass, and $r_0 \sim 10^7$ cm is the radius of the jet base, implying an optical depth $\tau = n\sigma_T r_0 \sim 0.001 - 0.01$. Since the optical depth is small, the probability of multiple Compton scattering is very small and we only consider single scattering. For the non-thermal power law electrons, the lower cutoff in the Lorentz factor is assumed to be equal to peak of the relativistic Maxwell-Jüttner distribution, i.e. $\gamma_{e,min} = 2.23kT_e/(m_e c^2)$.

Following the prescription of Falcke & Biermann (1995); Falcke (1996) for maximally efficient jets, we assume that the bulk speed of the plasma (with adiabatic index $\Gamma = 4/3$) at the base of the jet is the sound speed given by $\beta_s = \sqrt{(\Gamma - 1)/(\Gamma + 1)} \sim 0.4$. We do not model the particle acceleration in the jet, but just start at the sonic point. Each jet then accelerates longitudinally along its axis due to pressure gradient and expands laterally with its initial sound speed. The bulk velocity profile, magnetic field strength, electron density and electron Lorentz factor along the jet are calculated by solving the adiabatic, relativistic Euler equation.

In the previous versions of the jet model (e.g. in Markoff et al. 2005) we used the ratio of scattering mean free path to gyroradius of the particles in the plasma through which the shock moves (f_{sc}), as a model parameter. However given the current lack of physical understanding of the actual shock propagation mechanism, in this paper we fixed the shock speed in the plasma (β_{sh}) to 0.6 and used the quantity $\epsilon_{sc} = \beta_{sh}^2 / (\text{ratio of scattering mean free path to gyroradius})$ as a model parameter instead of f_{sc} . The parameter ϵ_{sc} can be physically interpreted to be a parametrization for the shock acceleration rate ($t_{acc} \propto \epsilon_{sc}^{-1}$; see eq.1 of Markoff et al. 2001). The dominant cooling processes within the jet are synchrotron and synchrotron self-Compton radiation. If the inner edge of the accretion disc is sufficiently close to the base of the jet, then the soft photons from the accretion disc, acting as seed photons for external Comptonization, can also cool the particles in the jet. The jet continuum as observed by an observer on Earth is a superposition of spectra from individual segments along the jet axis (taken to be perpendicular to the accretion disc plane), calculated by solving the radiative transfer equation, after taking into account relativistic beaming effects.

3.2 The irradiated disc

Since the coupling between disc and jet is not well understood, we assume an independent classical thermal viscous ‘‘Shakura-Sunyaev’’ accretion disc, with a radial temperature profile $T(R) \propto R^{-3/4}$, and modeled by the parameters T_{in} , r_{in} , the temperature and radius at the inner edge of the disc. If the outer parts of the disc are irradiated, then as discussed below, it is further possible to constrain the temperature and radius at the outer edge of the disc. Given the mounting evidence for the existence of relativistic outflows from black holes, we also explore the influence of the jet acting as a source of irradiation heating of the accretion disc.

3.2.1 Can jets influence the energetics of the accretion disc ?

We computed the radiative jet flux incident on the accretion disc as a function of radial distance on the disc plane, taking into account special relativistic beaming effects. In order to obtain an *upper limit* on the jet-induced heating of the accretion disc, we assumed that the entire incident radiative flux from the jet $f_v(R)$ is thermalized upon being absorbed by the disc, thus heating the disc locally at radius R at a rate $H_{jet}(R)$, given by

$$H_{jet}(R) = \int_0^\infty f_v(R) dv \quad (1)$$

We calculated $H_{jet}(R)$ at ten logarithmically spaced radii spanning from R_{in} to R_{out} . The ratio of $H_{jet}(R)$ to the local viscous heating ($H_{visc}(R)$) is shown in Fig. 1. At large radii ($R > 100 R_g$), $H_{jet}(R)$ has a $\sim r^{-2.4}$ radial profile, which is somewhat steeper than that expected from irradiation by a static corona or the inner accretion disc (for which the irradiation heating falls as $\sim r^{-1.6}$ to -2.0 ; see, e.g., §3.2.2 and Hynes (2005)). However the local viscous heating rate drops outward even faster ($H_{visc}(R) \propto R^{-3}$), thus causing the ratio $H_{jet}(R)/H_{visc}(R)$ to slowly increase for increasing R . As the disc radius becomes small and approaches that of the jet base, the solid angle subtended by the jet increases rapidly causing the jet heating to saturate. However the viscous heating continues to rise at smaller radii and causes $H_{jet}(R)/H_{visc}(R)$ to drop at small radii. However, as evident from Fig. 1, even the maximum possible jet-induced heating of the disc is about seven orders of magnitude smaller than the viscous heating. This confirms that relativistic beaming of the jet causes a very small fraction of the flux emitted by the jet to fall back on the disc, and the resulting influence of the jet on the energetics of the disc is negligible.

Light bending effects near the black hole can enhance the flux incident on the disc, but by not more than a few tens of percent of the numbers calculated above (i.e. by assuming Minkowski metric instead of a more realistic Kerr or Schwarzschild metric).

3.2.2 An irradiation source near the compact object

Analysis of OIR light curves of XTE J1118+480 by Zurita et al. (2006) suggests there might have been significant contribution of thermal flux in the optical. The near-IR flux however is reported to be significantly non-thermal in nature from studies of rapid time variability in the light curve, as well as nearly flat IR SED (Zurita et al. 2006; Hynes et al. 2006). As discussed in the previous paragraph as well as shown in Fig. 1, the jet’s contribution in heating the disc is negligible; we have therefore added an irradiation heating term due to a somewhat more static source of irradiating X-rays near the black hole. The physical origin of this irradiating source could be the inner accretion disc near the black hole. Since we assume a radial temperature profile and do not solve the local disc structure (which in itself is a detailed MHD problem, see, e.g., Hawley et al. 2007, and references therein), our model cannot discern the source of the irradiating X-rays.

The temperature due to irradiation heating (T_{irrad}) is usually assumed to have a power law radial dependence of the form R^{-n} . Depending on the initial assumptions about disc structure and geometry of the irradiating source, theoretical models predict n to be in the range of 0.4-0.5 (Vrtilek et al. 1990; King et al. 1997; Dubus et al. 1999). Given the uncertainties in de-reddening and scarcity of data points in the OIR, the exact choice of n is not vital for a global understanding of the broad-band SED. We used $n = 3/7$ (vertically isothermal disc with disc height $h \propto r^{9/7}$), mainly for consistency with earlier work (e.g. by Vrtilek et al. 1990; Hynes et al. 2002; Hynes 2005).

We assume that the total disc heating is a sum of local viscous heating, and heating due to a static source of irradiation near the black hole. The effective temperature of the disc (T_{eff}) is therefore related to the viscous temperature (T_{visc}) and the irradiation temperature (T_{irrad}) as follows:

$$T_{eff}^4(R) = T_{visc}^4(R) + T_{irrad}^4(R), \quad (2)$$

where $T_{\text{visc}} = T_{\text{in}}(R/R_{\text{in}})^{-3/4}$ and $T_{\text{irrad}} = T_{\text{out}}(R/R_{\text{out}})^{-3/7}$ with $T_{\text{in/out}}$, $R_{\text{in/out}}$ as free parameters. Other parameters, viz. masses, inclination and distance to the binary system, are taken from values published elsewhere and kept fixed during the process of fitting. The radius R_{irrad} where irradiation heating becomes equal to viscous heating can be estimated from

$$R_{\text{irrad}} = \left[(T_{\text{in}}/T_{\text{out}}) R_{\text{out}}^{-3/7} / R_{\text{in}}^{-3/4} \right]^{28/9}. \quad (3)$$

Since viscous dissipation dominates for $R < R_{\text{irrad}}$, the disc height at R_{irrad} is estimated from Shakura-Sunyaev's α -disc solution (see e.g. Shakura & Sunyaev 1973; Frank et al. 2002) as

$$H(R_{\text{irrad}}) = 1.7 \times 10^8 \alpha^{-1/10} \dot{M}_{16}^{3/20} (M/M_{\odot})^{-3/8} R_{\text{irrad};10}^{9/8} f^{3/5} \quad (4)$$

where we have $\dot{M}_{16} = \dot{M}/(10^{16} \text{ g/s})$, $R_{\text{irrad};10} = R_{\text{irrad}}/(10^{10} \text{ cm})$, $f = [1 - 2GM/(c^2 R_{\text{irrad}})]^{1/4}$ and chosen $\alpha = 0.05$. Similarly, since $H \propto R^{9/7}$ when $R > R_{\text{irrad}}$, the disc height at R_{out} is given by

$$H(R_{\text{out}}) = H(R_{\text{irrad}}) \times (R_{\text{out}}/R_{\text{irrad}})^{9/7}. \quad (5)$$

The solid angle subtended by the outer, irradiation dominated disc as seen from the compact object is computed from equations 4 and 5.

The *agnjet* model computes the broadband continuum from the jet and the irradiated disc but not line emission or reflection features. Therefore we used an additional Gaussian line profile to fit the iron $K\alpha$ emission complex near 6.5 keV and the convolution model *reflect* (Magdziarz & Zdziarski 1995) for the excess in the range of 10–30 keV, both features being usually attributed to reflection by the relatively cold accretion disc. The column density, taken from elsewhere published values, was fixed during the fits. For the *reflect* model, which accounts for reflection from neutral material in the accretion disc, we used solar abundance and tied the inclination to that of the disc (and also the jet axis). The energy of the iron line in the Gaussian model was allowed to vary between 6–7 keV and its width was fixed to 0.5 keV. The spectral coverage, along with column density (N_{H}) towards the sources, distances, and masses of the compact objects are given in Table 1.

3.3 Model fits

Spectral fittings were performed using *ISIS* (v1.4.9-4; Houck 2002). Evaluation of confidence intervals for any physical model is computationally expensive, and this is true for *agnjet* model as well. Therefore we have used the parallelization technique described in Noble et al. (2006) and distributed the task of computing confidence intervals³ for f free parameters over $f/2$ or $(f + 1)/2$ nodes (depending on whether f is even or odd; each node is an Intel Xeon 3.4GHz processor) of a Parallel Virtual Machine (Geist et al. 1994) running on the LISA cluster in Almere, Netherlands. This reduced the runtime to under 24 hours, a greater than 75% speedup; it also allowed us to discern finer features in parameter space by increasing the tolerance resolution by a factor of 500, while keeping the overall runtime to approximately half the serial runtime of 96 hours. While these are welcome improvements, reducing the model runtime even further would enable us to analyze new data more quickly. For this reason we are experimenting with ways of utilizing more than one processor per parameter, such as partitioning parameter space more finely, and exploring the use of OpenMP

(Dagum & Menon 1998) to parallelize internal loops within the model source code.

Using the distributed parallel computing technique described above, we determined the best-fit parameter values as well as their confidence intervals. Our confidence intervals correspond to $\Delta\chi^2 = 2.71$ for a given parameter (which for *normal* distribution would imply a 90% single parameter confidence limit).

3.3.1 XTE J1118+480 during 2005 outburst

Of the three data sets presented in this work, the data from the 2005 outburst of XTE J1118+480 was the faintest and had a steep power law slope in the X-rays. The flux in the HEXTE bands was extremely low for this data and while regrouping the data we found that no flux with $S/N > 4.5$ could be detected above 60 keV. Since the single point in the radio frequency does not constrain the length of the jet, we fixed it to $10^{13.1}$ cm which is a lower limit on the radiative length of the jet assuming that the radio data point is still on the optically thick synchrotron regime with a flat-to-slightly-inverted spectral index. While the fits require a high fraction of non-thermal electrons in the post-shock jet (> 0.5), they are not very sensitive to the exact value of this fraction, and we fixed its value to 0.75. The data cannot be described by a non-thermal jet continuum alone and an excess in the OIR data requires additional flux which we modeled using the irradiated accretion disc model described in §3.2. This thermal excess in the optical has also been suggested from the OIR coverage of the outburst by Zurita et al. (2006) and Hynes et al. (2006).

The X-ray data (3–60 keV) can be well fit ($\chi^2/\nu = 88.8/55$) only with a power law, however systematic residuals in the 5–7 keV range suggest that a weak iron line may be present. Adding a Gaussian line to the power law improves the fits to $\chi^2/\nu = 79.5/52$, with the line center near 6.6 keV and width of 0.1 keV. Given the weak strength of the lines, we fixed the line energy as well as the width to these values, and did not use any reflection model modeling the broad band SED of XTE J1118+480.

Fits performed by allowing r_{in} and T_{in} of the accretion disc to vary freely results in good fits with quite small values of both r_{in} and T_{in} . There are uncertainties in our understanding of the physical properties of the innermost regions of the disc close to ISCO, dereddening of interstellar extinction, and also uncertainties in instrumental response and calibration. These concerns make detection of a cold disc with small r_{in} , T_{in} and its physical origin open to debate (Miller et al. 2006a,b; Rykoff et al. 2007; Ramadevi & Seetha 2007; Gierliński et al. 2008; D'Angelo et al. 2008; Reis et al. 2009). Another issue with the XTE J1118+480 data is the jet/disc inclination. While we usually fix the inclination to a value published elsewhere, the extremely flat radio to IR spectrum of XTE J1118+480 requires a much smaller inclination than the published value of $\sim 70^\circ$ (see, e.g., Gelino et al. 2006; Chaty et al. 2003; McClintock et al. 2001; Zurita et al. 2002). Allowing the inclination to vary for this source results in jet inclination of $\sim 25^\circ$.

Therefore we tried two different models for this data set of XTE J1118+480. In the first model (Model 1; second column in Table 2), apart from other regular parameters described above, the jet/disc inclination as well as r_{in} and T_{in} were allowed to vary freely. In the second, somewhat more conservative model (Model 2; third column in Table 2), the jet inclination was fixed to 30° , r_{in} , T_{in} were also fixed to $30 R_g$ and 0.1 keV respectively. The best-fit values for the second model also gives similar jet parameters as the first model, although with a slightly higher jet power and steeper elec-

³ Using our own custom versions of the *c1_master* and *c1_slave* scripts described at http://space.mit.edu/cxc/isis/single_param.conf_limits.html

tron distribution index. Also the second model favors a somewhat smaller and hotter outer disc edge.

3.3.2 XTE J1118+480 during 2000 outburst

We used the broadband SED data of XTE J1118+480 obtained around 2000 April 18, published in McClintock et al. (2001) and Hynes et al. (2000). While analyzing this data set a broad dip in the combined EUVE and Chandra spectra was noted between 0.15–2.5 keV (see e.g. the residuals in Fig. 3) which cannot be modeled using the standardly used column density for this source ($1.3 \times 10^{22} \text{ cm}^{-2}$). This feature was been noted by previous works as well, and is attributed to metal absorption in a partially ionized gas, (see e.g. Esin et al. 2001). We have therefore excluded the energy range between 0.15–2.5 keV from our broadband fitting. Results of fitting indicate that during this observation emission from the jet dominates the radio and IR regions. Contribution from the accretion disc starts becoming dominant in the optical. However, as discussed in Hynes et al. (2000), the EUVE fluxes are extremely sensitive to the extinction law, and the slope of the dereddened EUVE SED can range between $+2 \geq \alpha \geq -4$ ($F_\nu \sim \nu^\alpha$) for the permissible range of N_H . Here we have used the EUVE fluxes reported by (Hynes et al. 2000; McClintock et al. 2001) and a column depth of $N_H = 1.3 \times 10^{20} \text{ cm}^{-2}$, which results in a very steep EUVE slope. This cutoff in the EUVE data would imply a cold, truncated inner disc with $r_{\text{in}} \sim 340 R_g$ and $T_{\text{in}} \sim 2.9 \times 10^5 \text{ K}$. Given the low temperature of the inner disc and the consequent absence of a irradiating soft X-ray photons, it is not unexpected that we do not find any signature of irradiation in this case (i.e. T_{out} is not constrained). As in the case of the 2005 data of this source, the X-ray emission in this model is entirely dominated by optically thin synchrotron emission from the jet. While the fits require a small nozzle ($h_0/r_0 \sim 0.2 - 0.6$), they are not very sensitive to the exact value of this parameter, and we fixed its value to 0.4. We note that this value is about a factor of three smaller than what is found typically in other sources, or even during the 2005 outburst of this source.

3.3.3 GX 339–4 during 2002 outburst

The X-ray data of GX 339–4 cannot be well fit by a power law alone. Using simple power law+ Gaussian model gives unacceptable fit to the data with reduced χ^2 of 5.9. Convoluting a power-law+gaussian with a reflection model give better fits, but still with rather a large reduced χ^2 of 2.3. We found that the GX 339–4 data can be fitted well without including any thermal component, and the entire broadband SED is well described by the superposition of synchrotron and inverse Compton photons from the pre-shock region near the jet base as well as optically thick synchrotrons from post-shock regions farther from the jet base. From the radio-IR slope, the required inclination is between 45–50 degrees, but not well constrained and hence was fixed at 47 degree. The length of the jet was fixed to $10^{14.2} \text{ cm}$ and fraction of non-thermal electrons fixed to 0.75 for the same reasons given for XTE J1118+480. Since the spectrum of GX 339–4 could be entirely dominated by jet emission, and the source was in a bright, hard X-ray state (Homan et al. 2005), the input jet power is much larger than that of XTE J1118+480. In fact the jet power for this observation is larger than any of the previous observations of this source (Markoff et al. 2003, 2005). Also the acceleration region starts much farther out for the GX 339–4 data set.

If the temperature of the thermal electrons (T_e) at the base is

left completely free, as in “Model 1” (fifth column in Table 2), then T_e for the best-fit model is comes out to be rather high, and suggests that the SED at energies $> 10 \text{ keV}$ is almost entirely due to SSC emission from the base (see top two panels in Fig. 4). The geometry of the base is rather compact and the source is in a bright hard state; therefore a strong SSC emission could imply that the photon density at the base becomes high enough for pair processes to become important. Since pair production is not included in the model, an estimate of the importance of pair processes for the best fit models were done as follows: the pair production rate (\dot{n}_{pp}) was calculated from the photon field at the base of the jet using the angle averaged pair production cross section (Gould & Schröder 1967; Boettcher & Schlickeiser 1997); pair annihilation rate (\dot{n}_{pa}) was calculated following Svensson (1982). For “Model 1” of GX 339–4, $\dot{n}_{pp} \sim 10^{17} \text{ cm}^{-3} \text{ s}^{-1}$ and $\dot{n}_{pa} \sim 10^{12} \text{ cm}^{-3} \text{ s}^{-1}$, suggesting that pair processes could be important in this case. Therefore we explored the parameter space, limiting the electron temperature to be less than $5 \times 10^{10} \text{ K}$ and somewhat less compact base (larger r_0, h_0) to search for solutions which also satisfy the condition $\dot{n}_{pp} < \dot{n}_{pa}$ (see “Model 2”, sixth column in Table 2 and bottom panels in Fig. 4). The fit derived number density (n), \dot{n}_{pa} and \dot{n}_{pp} for the different models presented in Table 2, are given in Table 3.

In addition to the continuum jet model, an additional Gaussian line centered at 6.3 keV and reflection from the accretion disc is needed to obtain good fits for the GX 339–4 data. Presence of the line and reflection suggests the presence of an accretion disc. However, as in the case for XTE J1118+480, the disc is cold and therefore not detected by the PCA.

The best-fit model parameters, associated confidence intervals, χ^2 statistic and corresponding chance probabilities for both sources are shown in Table 2. Given the simplicity of the model it is hardly unexpected that the reduced χ^2 values obtained from the fitting are not very close to 1 in some cases. For instance, the viscous+irradiated disc model does not include details of disc atmosphere or ionization balance equations, and is therefore not able to predict the spectral breaks in the optical data. Because of its simplicity, this is not meant to be a real model of the disc, although it incorporates the dominant ongoing physical processes and can reproduce the general shape of the broadband continuum. Moreover, while fitting a data set spanning 10 decades in frequency (or energy) space, the long lever arm between radio and X-rays constrains the jet model more strongly than the overall chi-squared (see e.g. Markoff et al. 2008). Best fit models along with data and residuals are shown in Figures 2, 3 and 4.

4 DISCUSSION AND CONCLUSIONS

We have analyzed broad band multi-wavelength observations of the galactic black hole transient systems XTE J1118+480 and GX 339–4, during their outbursts in 2000 and 2005 for XTE J1118+480, and during the 2002 outburst of GX 339–4. The conclusions from our study are summarized below.

The data for XTE J1118+480 cannot be fit well with a jet continuum model alone, due to an excess in the OIR fluxes. During these observations, in OIR the source was at least 3.5 magnitude brighter than quiescence; therefore the contribution from the M1 V secondary star (Chaty et al. 2003, and references therein) is small. Modeling the data from the 2000 outburst and 2005 outburst of this source we found that the outer disc was strongly irradiated during the 2005 data. It appears that the inner edge of the accretion disc

was much closer to the central black hole during the observations of 2005, thus providing an ample source of soft X-ray photons to irradiate the outer disc. On the other hand, the sharp cutoff in the EUVE data and absence of any signature of irradiation from the outer disc suggests a recessed, cold accretion disc for the 2000 data. However, as discussed in §3.3.2, the slope of the EUVE data depends very strongly on the assumed column depth, and a small decrease in N_H can flatten the EUVE SED significantly (see e.g. Hynes et al. 2000). Such a flat EUVE SED would be expected from a disc with small r_{in} and comparatively higher T_{in} (Reis et al. 2009).

Our calculations in §3.2.1 show that at any point on the surface of the accretion disc, the heating of the disc by the jet is seven or more orders smaller than the viscous heating. There are two factors which largely reduce the amount of jet radiation that is incident on the disc: Firstly Doppler de-beaming - since the bulk motion of the jet is relativistic, special relativistic Doppler beaming concentrates most of the emergent radiation from the jet in the direction of its motion, i.e. away from the disc. A second, but significant factor that also contributes to the diminution of jet flux incident on the disc is the fact that the post-shock jet synchrotron spectra peaks at increasingly longer wavelengths at increasingly larger distances from the base of the jet, thus creating fewer X-ray photons that can heat the disc. This is illustrated in Fig. 1 where we show the ratio of jet-heating to viscous heating as a function of radius. Since heating by the jet alone cannot produce the OIR excess in Fig. 2 we surmised that this the OIR excess is indeed caused by the more conventional form of irradiation, i.e. irradiation by soft X-ray photons from the inner-disc. From an energetics point of view, it is easy to see that the inner accretion disc alone (see Fig. 2, at around 1 keV) radiates at least two orders or more energy than the outer region. Furthermore, it is well known that the outer edge of the accretion disc can flare-up or warp (e.g. Ogilvie & Dubus 2001), thus making the outer parts of the disc more easily visible from the inner regions.

Fits to the 2005 data of XTE J1118+480 using the jet model+irradiated disc (described in §3.2.2) suggest a cold disc ($T_{in} \sim 0.2$ keV) with inner radius close to the innermost stable circular orbit ($6 R_g$ for a Schwarzschild black hole, and smaller if spinning). Given the uncertainties associated with using a simple $T \sim R^{-3/4}$ model which ignores correction factors like spectral hardening (Shimura & Takahara 1995), full disc structure as well as proper boundary conditions at the inner edge (Zimmerman et al. 2005), the errors associated with the estimates of the inner disc parameters are most likely an underestimate. Another source of uncertainty comes from that fact that we assume the jet to be perpendicular to the disc. A misaligned jet (Maccarone 2002), as seems likely for XTE J1118+480, could introduce additional error in the determination of r_{in} . Along with the uncertainties in instrument calibration, modeling and jet-disc alignment, the sharp low energy cutoff of PCA sensitivity below 3 keV makes detection of a cold disc with small r_{in} even more difficult than a recessed cold disc. Nevertheless the numbers for r_{in} and T_{in} we obtained for XTE J1118+480 are similar to those obtained by several others for black hole transients in their hard state (e.g. Di Salvo et al. 2001; Miller et al. 2006a,b; Ramadevi & Seetha 2007; Rykoff et al. 2007; Reis et al. 2009). If such a cold disc with small r_{in} is indeed realised, then Compton scattering of the disc photons could be strongly anisotropic, with most of the scattered emission beamed toward the disc (Henri & Petrucci 1997). This could compensate partly the beaming effects due to the relativistic motion of the gas, and increase the illumination of the disc (both irradiation and reflection effects). Also in this case there could be a radiative feed-

back due to the local illumination of the disc by the base of the jet which is similar to the situation in standard accretion disc corona models (Haardt & Maraschi 1993) which would act as a thermostat keeping the temperature at the base lower than what is assumed here. A somewhat more conservative model, where the temperature and radius of the inner edge of the accretion disc were fixed to 0.1 keV and $30 R_g$ respectively (Model 2 in Table 2) also describes the data well, showing the difficulty in detecting a cold disc with small r_{in} from the available data.

The best-fit outer radii of XTE J1118+480 for both *Model 1* and *Model 2* are smaller than the circularization radius, using the latest values of orbital parameters published by Gelino et al. (2006). These results are therefore consistent with the assumption that accretion is occurring via Roche lobe overflow. The observation was made during the decline from outburst peak. Hence the discrepancy between the circularization radius and R_{out} inferred from fits, in the context of standard disc instability models, could be due to an inward moving cooling wave. A decreasing trend in the outer radiative disc radius was also observed by Hynes et al. (2002) for the system XTE J1859+226. However the value of R_{out} in our case depends largely on the five OIR data points, all of which lie on the Rayleigh-Jeans region of the irradiated disc. Given the plethora of spectral features seen in OIR spectra of X-ray binaries in outburst (see, e.g., Hynes 2005; Charles & Coe 2006), the limitation of using a few bands is obvious.

Analysis of the data from the 2000 outburst of XTE J1118+480 by Esin et al. (2001) and Yuan et al. (2005) showed that the UV and higher energy data can be explained by an ADAF model. The flux from the ADAF model alone however falls sharply at energies below optical and underestimates IR and any lower energy data (e.g. radio), thus requiring an additional jet component (Yuan et al. 2005; Narayan & McClintock 2008). In the jet-ADAF model (Yuan et al. 2005), the X-ray photons have a thermal Comptonization origin, whereas in the current work, the X-ray photons can originate from either synchrotron (e.g. in XTE J1118+480), or inverse Compton scattering, or a combination of both (e.g. in GX 339-4). Better simultaneous broadband coverage and future X-ray polarization studies can help to estimate the relative importance of these two emission components which dominate the X-ray spectra of X-ray binaries in hard state.

From the available data, the X-ray spectrum of XTE J1118+480 during both outbursts show little or no curvature at energies higher than ~ 10 keV. Reflection features like the iron line complex and the reflection ‘‘bump’’ near 20 keV are also extremely weak. Detailed analysis of the X-ray spectra taken by Chandra and RXTE, during the 2000 outburst of this source by Miller et al. (2002) also showed extremely weak reflection features, as would be expected for a jet+recessed disc scenario. From a phenomenological point of view, since the curvature is small, using a broken power law to describe data of X-ray binaries in hard state has been shown to work remarkably well, e.g., for GX 339-4 by Nowak et al. (2005) and for Cyg X-1 by Wilms et al. (2006). Residuals of a power law fit to the X-ray continuum in the 2005 data set of XTE J1118+480 show small systematic variations near 5-7 keV, which improves slightly upon addition of a Gaussian line. However, given the weakness of the line, its energy or width cannot be constrained well. Total contribution from various source of inverse Comptonization (SSC within the jet base and external Comptonization of soft thermal photons from the accretion disc) is also much smaller compared to that of GX 339-4. The X-ray region of the SED of XTE J1118+480 is dominated by post-shock synchrotron photons for both 2000 and 2005 outbursts. We note

that the electron acceleration region seems to be in the nozzle of the jet in the case of 2005 outburst data of XTE J1118+480 while it is farther out in the jet in GX 339–4 as well as the 2000 outburst of XTE J1118+480. While exhaustive searching of the χ^2 space confirms that this is required by the data, it is not clear why the acceleration region is inside the nozzle for the 2000 data of XTE J1118+480. Another unexpected result is that the base of the jet seems to be quite small ($h_0/r_0 \sim 0.4$) for the 2000 outburst data of XTE J1118+480, whereas $h_0/r_0 \sim 1.5$ for other outbursts of XTE J1118+480 as well as other sources (see e.g. Markoff et al. (2005); Gallo et al. (2007); Migliari et al. (2007)). Given the uncertainties in our understanding of jet formation and the acceleration region, and the simplicity of the model, here we report the best fit parameters as obtained. The particle energy distribution index (p) of the relativistic post-shock electrons for data from both outbursts of XTE J1118+480 is ~ 2.5 – 2.6 . This value is much steeper than what could be expected from an initial distribution of particles accelerated by a diffusive shock process (~ 1.5 – 2 ; Heavens & Drury 1988). However it is possible that for XTE J1118+480 the observed X-ray bandpass is at a higher energy than the cooling break energy, where the particle distribution steepens from p to $p + 1$ due to enhanced cooling. One of the key assumptions in our model is time independence of particle distributions. However if the steep power law drop-off of the observed photon index is indeed due to enhanced cooling, or more generally a departure from the assumed equilibrium between the heating and cooling processes, a more thorough time dependent analysis of particle evolution is necessary. We will present time dependent particle evolution in the context of jets in a forthcoming paper.

The jet inclination of XTE J1118+480 is still a matter of concern. The optically measured system inclination is near 70° (Gelino et al. 2006; Chaty et al. 2003; McClintock et al. 2001; Zurita et al. 2002). However, given the flat radio-to-IR fluxes, jet inclinations higher than $\sim 30^\circ$ would be very difficult to fit which might suggest a large misalignment between between the disc and the jet (Maccarone 2002). Evidence of misalignment between disc and jet has been seen in several stellar X-ray binary systems, e.g., GRO J1655–40 (Greene et al. 2001; Hjellming & Rupen 1995), SAX J1819–2525 (Hjellming et al. 2000; Orosz et al. 2001), XTE J1550–564 (Hannikainen et al. 2001; Orosz et al. 2002), as well as in several AGNs, e.g., NGC 3079 (Kondratko et al. 2005), NGC 1068 (Caproni et al. 2006) and NGC 4258 (Caproni et al. 2007). Allowing the inclination to vary for XTE J1118+480 during the fits gives a best-fit inclination of $\sim 25^\circ$, and it is almost impossible to find statistically good fits (e.g. with $\chi^2/\nu < 2$) for inclinations larger than 30° . Previous fits by Markoff et al. (2001) also required a similar, small inclination. In our model we assume the lateral expansion and longitudinal acceleration of the jet to be driven solely via the solutions of the relativistic Euler equation for adiabatic expansion. If this is not the case, and e.g. the jet radius and acceleration are determined by some other process(es) leading to a stronger magnetic field and/or smaller bulk velocity along the jet, that could lead to a flatter radio-IR spectrum as well (also see the discussion in §3.3.3 of Migliari et al. 2007).

The data for GX 339–4 does not formally require a thermal component (e.g. an accretion disc or emission from the secondary star) and the entire broad band emission from radio to X-rays is satisfactorily well fit by non-thermal photons originating from pre- and post-shock synchrotron, and synchrotron self Compton emission mainly from the jet base. Previous fits to the 3–100 keV X-ray data by Homan et al. (2005) also suggested that the disc contribu-

tion within this energy range is $\sim 1\%$ of the total luminosity or less. However presence of the line near 6.5 keV and signature of reflection suggests a cold accretion disc near the black hole which cuts off exponentially at an energy significantly below the lower detection limit of the RXTE/PCA. Since the X-ray spectrum has a luminosity of $\sim 5\% L_{\text{Edd}}$, the disc luminosity is presumably $\sim 0.05\% L_{\text{Edd}}$ or smaller.

The data for GX 339–4 were taken when the source was in a bright, X-ray hard state (Homan et al. 2005). The jet power N_j is much higher than that obtained by Markoff et al. (2005), who studied data from previous outbursts of the same source. We also obtain a higher equipartition factor (k) and shallower particle distribution index. It is interesting to note that r_0 and z_{acc} for GX 339–4 are always found to be higher than those found for other sources. If the electron temperature at the base is left unconstrained (e.g. “Model 1” in the fifth column of Table 2), then the density of photon field from best-fit model is high enough that pair processes may become important. In this case many photons are up-scattered above the pair production threshold, and the rate at which pairs are produced is much larger than the rate at which they are annihilated, thereby changing the density at the base of the jet. Constraining the electron temperature to be less than 5×10^{10} K, we present another fit (“Model 2”, sixth column of Table 2) where the photon density at the base is small and pair production rate is much smaller than the pair annihilation rate. For this fit the fractional pair annihilation rate (\dot{n}_{pa}/n) is also much smaller than unity, so that pair processes are not important for this fit.

Using the irradiated disc+jet model presented in this paper we have shown that in certain cases (e.g. the 2000 outburst data of XTE J1118+480) there are not enough X-ray photons from the inner regions to irradiate the disc appreciably. The 2005 outburst data of XTE J1118+480 presents an intermediate case where the contribution from an irradiated outer disc is comparable to the jet emission in OIR. The 2002 data of GX339–4 presents the extreme case where the entire broadband SED is dominated by emission from the jet.

The jet model has been used to analyze broad band SEDs of the stellar mass black holes XTE J1118+480 (Markoff et al. 2001, this work), GX 339–4 (Markoff et al. 2005, this work), Cyg X-1 (Markoff et al. 2005), A0620-00 (Gallo et al. 2007), GRO J1655-40 (Migliari et al. 2007), as well as that of the supermassive black holes in the nucleus our own galaxy (Sgr A*; Markoff et al. 2007) and that of M81 (Markoff et al. 2008). From the analysis of the spectra of these sources we note that the geometry of the jet base, scaled in units of gravitational radius, does not vary largely. The radius of the jet base, R_0 , lies in the range of 10–100 R_g , and the ratio of h_0/r_0 at the nozzle lies within 0.4–11, both suggesting a relatively compact jet base and the universal nature of mass scaling in accretion onto compact objects. The fraction of particles accelerated to a power law distribution beyond z_{acc} , while not very well constrained by the fits, prefers a value in the range of 0.6–0.9 and is fixed to 0.75. Considering that most of the known acceleration mechanisms in astrophysics do not have such a high efficiency, this number seems rather high and requires further exploration. The particle acceleration index (p) lies within 2.2–2.7, which is steeper than that expected from a relativistic shock (Heavens & Drury 1988, 1.5–2, see, e.g.), suggesting that in these cases the X-ray energies may lie beyond the *cooling break* (Kardashev 1962), so that the power law index of observed SED steepens by an additional amount of 0.5.

The magnetic-to-particle energy densities at the jet base (k) is often found to be greater than unity. MHD simulations of relativis-

tic jet launching (McKinney & Gammie 2004; Nakamura & Meier 2004; De Villiers et al. 2005; Fragile & Meier 2008) suggest that near the jet base, close to the launching points, the jets are mostly Poynting flux dominated and have small plasma fractions (ratio of gas pressure to magnetic pressure is less than unity). We are focusing on inner regions where this is likely still to be the case. In GRBs and AGN, most data is only relevant to regions well beyond the magnetosonic fast points, where the flow has been driven towards equipartition via conversion of magnetic energy to particle energy.

Temperature of the thermal electrons at the jet base (T_e) is in the range of $2 - 7 \times 10^{10}$ K for the stellar black holes and $\sim 10^{11}$ K for the supermassive black holes. The flow near the jet base could be a radiatively inefficient accretion flow (RIAF), i.e. an ADAF (Narayan et al. 1995; Rees 1982; Shapiro et al. 1976), or in light of the the magnetic domination, an MDAF (Meier 2005). In such a case, the ion temperature can be as high as the virial temperature, and electrons at 10^{9-10} K (Shapiro et al. 1976; Narayan et al. 1996). Keep in mind that for an outflow model, the particles are also not required to be gravitationally bound, and processes in the jet launching can heat the particles beyond virial, in theory.

Most likely the similarity in the derived physical parameters among the diverse sources and their diverse accretion states is not coincidental, and may hint towards an inherent similarity in the process of formation and propagation of compact jets. The results presented above show the importance of quasi-simultaneous, multi-wavelength, broad band SEDs in constraining geometrical and radiative parameters associated with accretion flows near compact objects.

Acknowledgements. This work was supported mainly by Netherlands Organisation for Scientific Research (NWO) grant number 614000530. JW acknowledges DLR grant 50OR0701. We would like to thank Guy Pooley for helping with the radio data, Michelle Buxton and Mickael Coriat for the OIR data reduction. We would also like to thank the anonymous referee for his/her constructive criticisms that have greatly improved the paper. DM thanks Asaf Pe'er for a discussion on pair processes in plasmas. It is a pleasure to acknowledge the hospitality of International Space Science Institute (ISSI) in Bern where a significant amount of this work was carried out.

This research has made use of data obtained from the High Energy Astrophysics Science Archive Research Center (HEASARC), provided by NASA's Goddard Space Flight Center. This work has also made use of the United Kingdom Infrared Telescope (UKIRT) which is operated by the Joint Astronomy Centre on behalf of the Science and Technology Facilities Council of the U.K. The Liverpool Telescope is operated on the island of La Palma by Liverpool John Moores University in the Spanish Observatorio del Roque de los Muchachos of the Instituto de Astrofísica de Canarias with financial support from the UK Science and Technology Facilities Council. We have also used radio data from the Ryle telescope operated by Mullard Radio Astronomy Observatory. Numerical computations for this work were done on the LISA workstation cluster, which is hosted by Stichting Academisch Rekencentrum Amsterdam (SARA) computing and networking services, Amsterdam.

	XTE J1118+480 (2000 outburst)	XTE J1118+480 (2005 outburst)	GX 339–4 (2002 outburst)
MJD of observation	51652	53393	52367-68
Spectral Coverage			
Radio:	15 GHz	15 GHz	5 GHz
UV,Opt/IR:	M, L, K, H, J-bands, EUVE and HST spectra	K, H, J, V, B-band	H, I, V-band
X-ray:	Chandra (0.24–7 keV), RXTE (3–110 keV)	RXTE (3–70 keV)	RXTE (3–200 keV)
N_{H} (10^{22} cm^{-2})	0.013	0.013	0.6
M_{BH} (M_{\odot})	8.5	8.5	7
Distance (kpc)	1.7	1.7	6

Table 1. Spectral coverage and source parameters used for the fits. For the 2000 outburst of XTE J1118+480 the radio data were obtained using the Ryle telescope, IR using the UKIRT, optical spectra using the HST, UV spectra using EUVE, X-ray spectra using Chandra and RXTE. The SED was constructed from data published in McClintock et al. (2001). For the 2005 outburst of XTE J1118+480 the radio data were obtained using the Ryle telescope, IR using the UKIRT and optical using the Liverpool telescope. The column density, mass of the black hole and distances were taken from the recent observations by Gelino et al. (2006) for the source XTE J1118+480. For GX 339–4, the SED was constructed from data published in Homan et al. (2005), black hole mass is lower limit by Muñoz-Darias et al. (2008), distance and column density from the ranges given by (Hynes et al. 2004).

Parameter (Unit)	XTE J1118+480 (2005 outburst; Model 1)	XTE J1118+480 (2005 outburst; Model 2)	XTE J1118+480 (2000 outburst)	GX 339-4 (2002 outburst; Model 1)	GX 339-4 (2002 outburst; Model 2)
N_j ($10^{-3} L_{\text{Edd}}$)	$2.32^{+0.02}_{-0.06}$	$2.77^{+0.01}_{-0.05}$	$7.2^{+0.1}_{-0.5}$	55^{+16}_{-9}	$83.8^{+0.2}_{-0.2}$
r_0 (R_g)	$9.39^{+0.18}_{-0.17}$	$11.8^{+0.1}_{-0.2}$	$20.8^{+1.0}_{-1.4}$	33^{+3}_{-2}	114^{+7}_{-11}
h_0/r_0	$1.589^{+0.013}_{-0.002}$	$1.39^{+0.03}_{-0.02}$	0.4★	$1.7^{+0.2}_{-0.1}$	$1.51^{+0.02}_{-0.03}$
T_e (10^{10} K)	$4.22^{+0.11}_{-0.02}$	$4.04^{+0.01}_{-0.02}$	$3.76^{+0.09}_{-0.07}$	$6.7^{+0.4}_{-0.5}$	$3.8^{+0.01}_{-0.2}$
z_{acc} (R_g)	$12.6^{+1.5}_{-0.0}$	$12.6^{+2.8}_{-0.0}$	$8.2^{+3.3}_{-0.2}$	252^{+212}_{-130}	526^{+85}_{-41}
p	$2.63^{+0.01}_{-0.01}$	$2.71^{+0.01}_{-0.01}$	$2.48^{+0.02}_{-0.01}$	$2.28^{+0.03}_{-0.03}$	$2.20^{+0.02}_{-0.01}$
ϵ_{sc} (10^{-3})	$9.9^{+0.02}_{-0.1}$	$29.9^{+0.3}_{-3.0}$	$5.5^{+1.4}_{-0.8}$	$0.16^{+0.08}_{-0.08}$	44^{+2}_{-1}
k	$1.9^{+0.1}_{-0.1}$	$2.3^{+0.1}_{-0.2}$	$2.1^{+0.1}_{-0.1}$	$2.2^{+1.4}_{-0.8}$	$2.38^{+0.01}_{-0.01}$
Inclination (deg)	$25.1^{+0.1}_{-0.0}$	30★	30★	47★	47★
r_{in} (R_g)	2.6^{+5}_{-0}	30★	341^{+4}_{-22}	Not constrained	Not constrained
T_{in} (keV)	$0.254^{+0.004}_{-0.008}$	0.1★	$0.025^{+0.001}_{-0.002}$	Not constrained	Not constrained
r_{out} (R_g)	15700^{+160}_{-350}	8850^{+1800}_{-1550}	29400^{+610}_{-5750}	Not constrained	Not constrained
T_{out} (K)	18100^{+1000}_{-600}	30500^{+200}_{-100}	650^{+2150}_{-550}	Not constrained	Not constrained
f (10^{-4})	1.2	1.0	Not constrained	Not used	Not used
E_{Line} (keV)	6.63★	6.63★	Not used	$6.3^{+0.2}_{-0.2}$	$6.3^{+0.3}_{-0.2}$
W_{Line} (eV)	39.3	27.7	Not used	93.5	58.7
$\Omega/2\pi$	Not used	Not used	Not used	$0.22^{+0.10}_{-0.14}$	$0.35^{+0.02}_{-0.02}$
χ^2/ν [Q]	70/50 [0.032]	90/53 [0.0011]	140/137 [0.406]	137/112 [0.054]	157/112 [0.0032]

Table 2. Best fit parameters for XTE J1118+480 and GX 339-4, and $\Delta\chi^2 < 2.71$ confidence intervals. A star (★) next to a number indicates that the parameter was frozen to that value. N_j = jet normalization; r_0 = nozzle radius; h_0/r_0 = height-to-radius ratio at base; T_e = pre-shock electron temperature; z_{acc} = location of acceleration region along the jet; p = spectral index of post-shock electrons; $\epsilon_{\text{sc}} = 0.36$ /ratio of scattering mean free path to gyroradius (see §3.1); k = ratio between magnetic and electron energy densities; Inclination = orbital inclination as seen from Earth (also the jet inclination); $r_{\text{in/out}}$ = radius of the inner/outer edge of the irradiated accretion disc; $T_{\text{in/out}}$ = temperature at the inner/outer edge of the irradiated accretion disc. While T_{out} is in Kelvin, T_{in} is reported in keV as is customary for X-ray observers; $f = (2\pi)^{-1} \times$ the solid angle subtended by the outer, irradiation dominated disc as seen from the inner disc; E_{Line} = energy of the iron K α line complex from the gaussian model; W_{Line} = equivalent width of the line; $\Omega/2\pi$ = reflection fraction from the reflect model. χ^2/ν is the reduced chi-squared and Q is the corresponding chance probability. For fitting the data of XTE J1118+480 from 2000, the energy range of 0.15 – 2.5 keV was excluded (see text, and also Esin et al. 2001). Also the disc inner edge parameters (r_{in} , T_{in}) are extremely sensitive to the extinction column depth (§3.3.2).

Source/Outburst/Model	$\log(n$ [cm^{-3}])	$\log(\dot{n}_{pa}$ [$\text{cm}^{-3} \text{s}^{-1}$])	$\log(\dot{n}_{pp}$ [$\text{cm}^{-3} \text{s}^{-1}$])
XTE J1118+480/2005/1	13.9	12.0	7.6
XTE J1118+480/2005/2	13.8	11.8	6.8
XTE J1118+480/2000	13.7	11.7	5.8
GX 339-4/2002/1	14.2	12.4	17.1
GX 339-4/2002/2	13.4	11.0	6.1

Table 3. The lepton number density (n), pair annihilation rate (\dot{n}_{pa}), and pair production rate (\dot{n}_{pp}) at the base of the jet for the various models presented in Table 2.

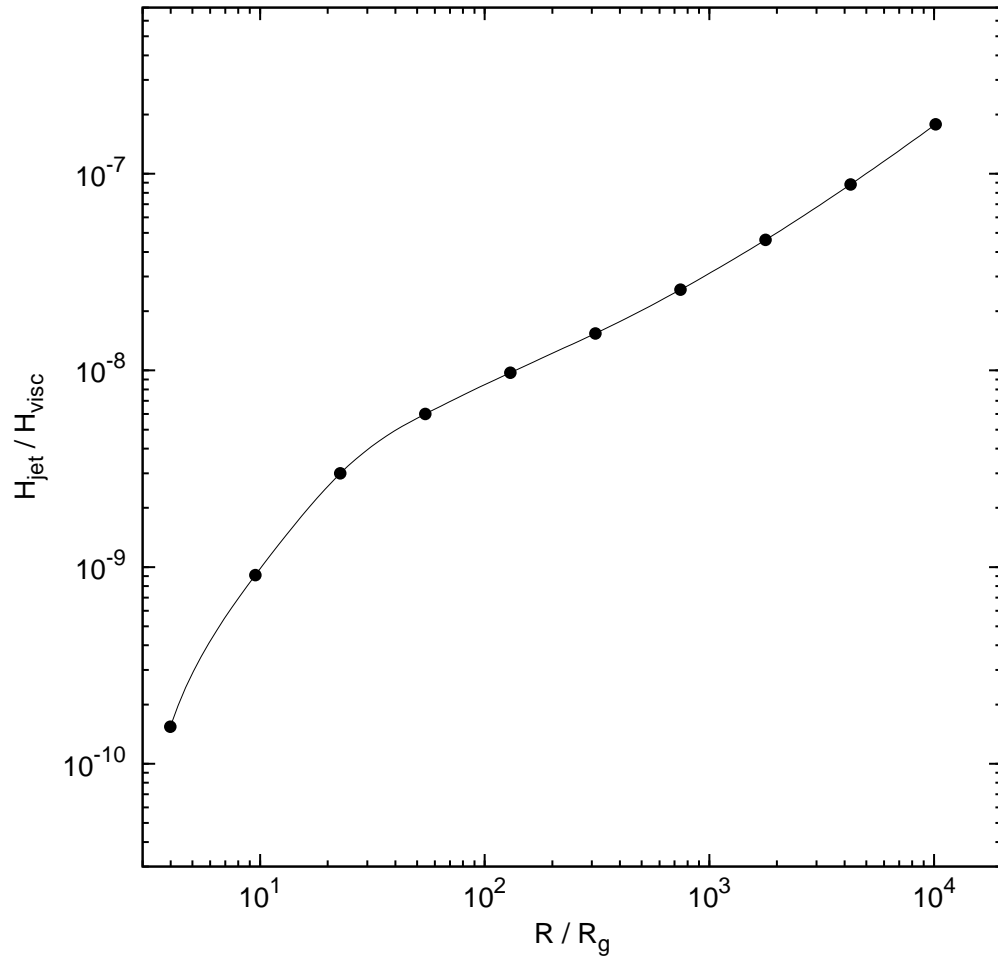


Figure 1. Comparing viscous heating (H_{visc}) and *maximum possible* “jet-heating” (H_{jet}) for XTE J1118+480. The filled circles are the computed upper limits of the ratio of jet induced heating to viscous heating ($H_{\text{jet}}/H_{\text{visc}}$), as discussed in §3.2.1, joined by a smooth spline. T_{in} , R_{in} and R_{out} for the disc were determined from broadband “Model 1” fits to the SED. For $R > 100 R_g$, the jet induced irradiation heating term falls more slowly ($\sim R^{-2.4}$) than the viscous heating ($\sim R^{-3}$), which causes the ratio $H_{\text{jet}}/H_{\text{visc}}$ to slowly increase at increasing radii. For $R_{\text{in}} < r_0$, the jet heating saturates but the viscous heating continues to increase for smaller radii, causing $H_{\text{jet}}/H_{\text{visc}}$ to drop sharply for decreasing radii.

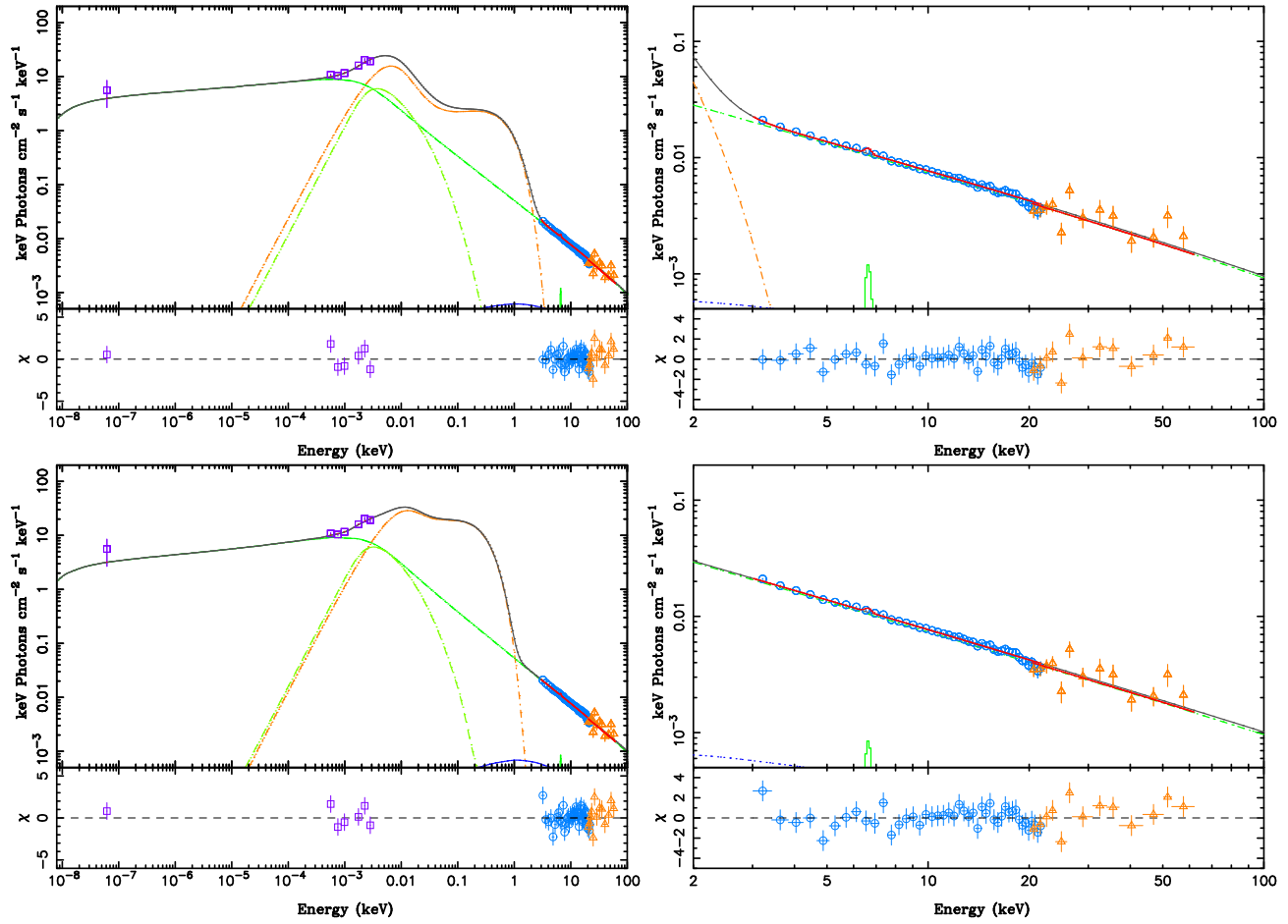


Figure 2. Jet model fits and residuals for the XTE J1118+480 data from its 2005 outburst. Left panels show the entire broad band SED from radio through X-rays, and a zoom of the X-ray region is shown in the right panels. Radio and IR data from the Ryle telescope and UKIRT respectively are shown by purple squares, RXTE/PCA data are shown by blue circles and RXTE/HEXTE data by orange triangles. The top panels are for “Model 1” in Table 2 (second column) where along with other parameters (see text), the jet inclination, r_{in} and T_{in} , were also allowed to vary. The value of the reduced chi-squared for best fit parameters of “Model 1” is 1.41. The bottom panels are for “Model 2” in Table 2 (third column) where jet inclination = 30° , $r_{\text{in}} = 30 R_g$ and $T_{\text{in}} = 0.1$ keV. The value of the reduced chi-squared for best fit parameters of “Model 2” is 1.69. The dark-green dash-dotted curve shows the post-shock synchrotron contribution, the green dashed curve shows the pre-shock synchrotron, blue dotted curve shows the Compton upscattered component. Flux from the irradiated accretion disc is shown by the orange dash-dotted curve. The solid grey line shows the total jet+disc model continuum spectrum without convolving through detector responses, interstellar extinction, the iron line or reflection. The iron line near 6.6 keV is shown by the thick, solid green line. The red line shows the properly forward-folded models taking into account detector responses, interstellar extinction, the iron line and reflection. Since interstellar extinction is small for XTE J1118+480, and the iron line and reflection features are very weak too, the forward-folded model (red line) is almost indistinguishable from the jet+disc model continuum (solid grey) in this figure as well as in Fig. 3. However for GX 339-4 (Fig. 4), where the iron line as well as reflection features are stronger, and the extinction is also larger, the difference between the unfolded and folded models (grey and red lines) becomes apparent.

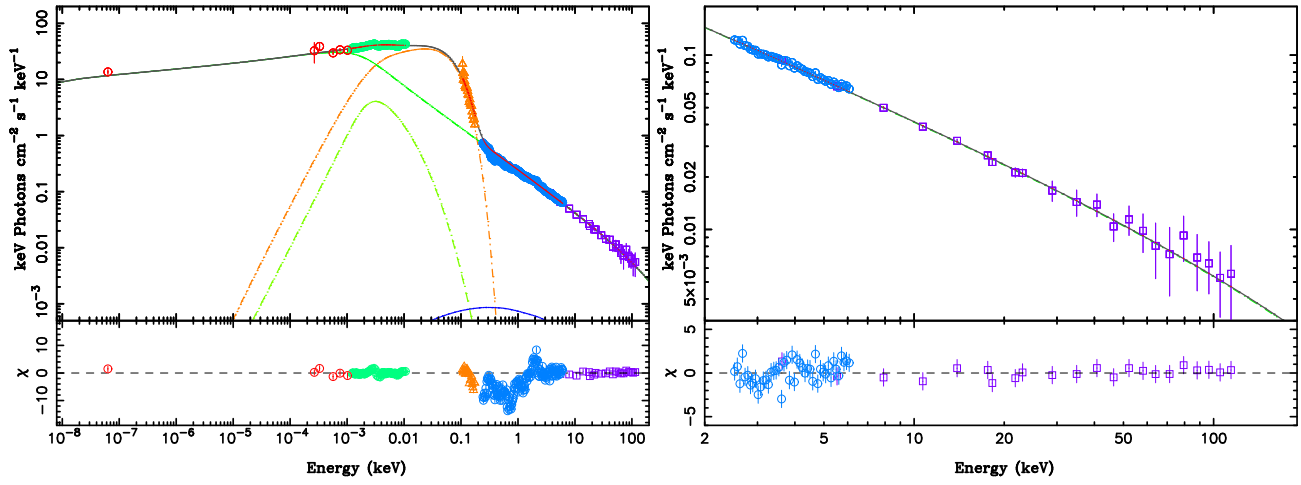


Figure 3. Jet model fits and residuals for the XTE J1118+480 data from its 2000 outburst (taken from McClintock et al. 2001) are shown in the left panel. The radio data from the Ryle telescope and IR data from UKIRT are shown by red circles, HST spectrum using green, EUVE data using orange triangles, Chandra spectrum using blue circles and RXTE data using purple squares. Note the dip in the 0.15–2.5 keV region which is attributed to the presence of a warm absorber (Esin et al. 2001). This region was excluded from our fits. A zoom of the X-ray region after excluding 0.15–2.5 keV data is shown in the right panel. The colour coding for the model components are the same as in Fig. 2.

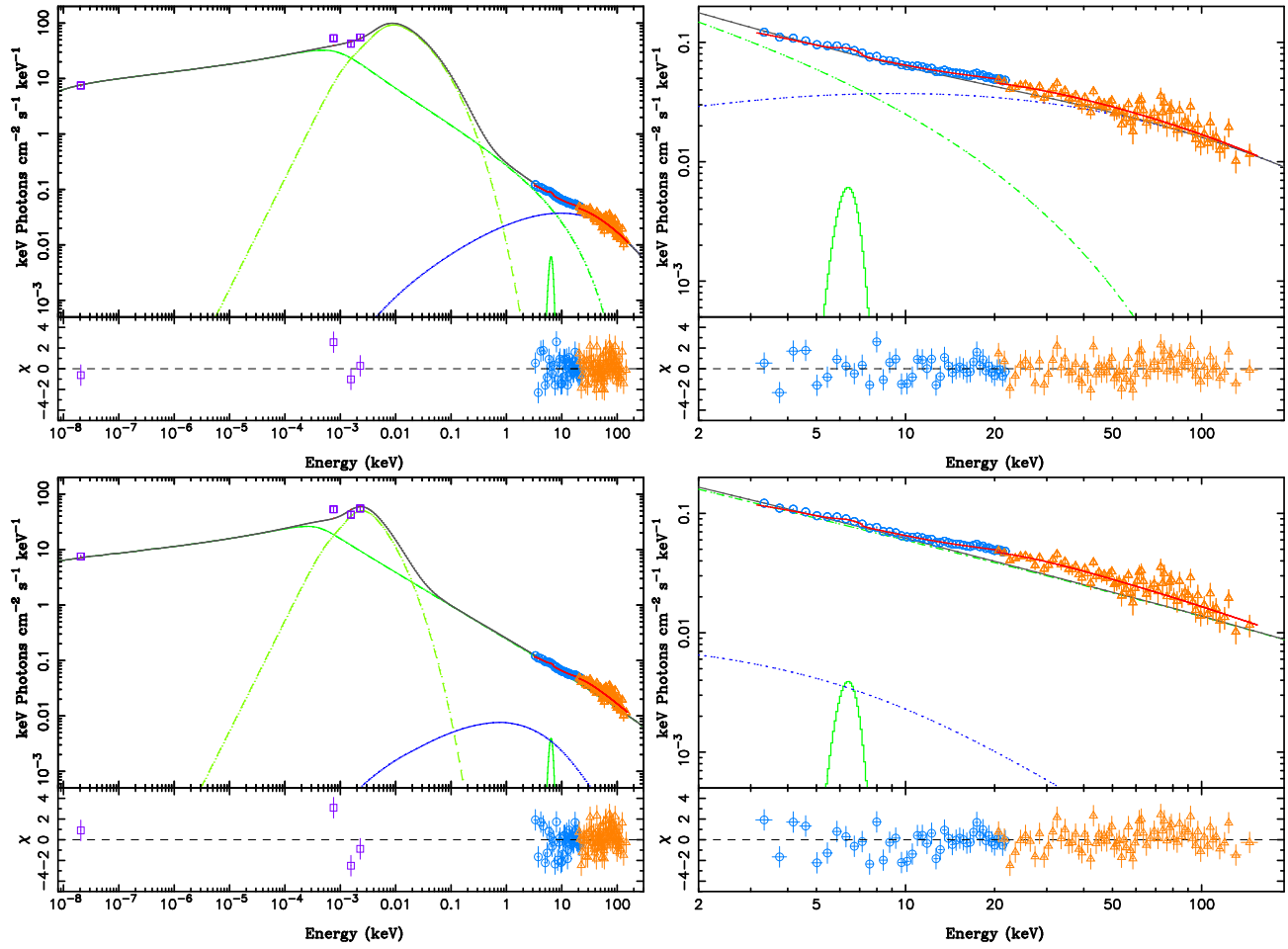


Figure 4. Same as Fig. 2, but for the source GX 339-4. The models presented here are purely jet models without any contribution from an accretion disc. The top panels are for “Model 1” (Table 2; fifth column) where along with other parameters the temperature of the thermal electrons at the base of the jet (T_e) was allowed to vary freely. The reduced chi-squared for this model is 1.22. Note the relatively strong inverse Comptonization component in the X-rays, originating at the jet base due to SSC emission in this model, compared to that in the case of XTE J1118+480. The bottom panels are for “Model 2” (Table 2; sixth column) where we constrained T_e to be less than 5×10^{10} K, reducing the SSC emission at the base. The base is less compact and acceleration starts farther out along the jet for “Model 2” compared to “Model 1”. The reduced chi-squared for this second model is 1.40. While the first model is a statistically better fit than the second, the photon density at the base can become high enough for pair processes to become important in the first model (see §3.3.3, §4 and Table 3), which is not the case for the second model. Also note the strong iron line near 6.3 keV and the reflection “bump” near ~ 20 keV, suggesting the presence of a cold accretion disc not detected at energies to which RXTE is sensitive.

REFERENCES

- Arnaud, K. A. 1996, in *Astronomical Data Analysis Software and Systems V*, ed. G. H. Jacoby & J. Barnes, ASP Conf. Ser. No. 101 (San Francisco: ASP), 17
- Blandford, R. D., & Königl, A. 1979, *ApJ*, 232, 34
- Boettcher, M., & Schlickeiser, R. 1997, *A&A*, 325, 866
- Bradt, H. V., Rothschild, R. E., & Swank, J. H. 1993, *A&AS*, 97, 355
- Caproni, A., Abraham, Z., & Mosquera Cuesta, H. J. 2006, *ApJ*, 638, 120
- Caproni, A., Abraham, Z., Livio, M., & Mosquera Cuesta, H. J. 2007, *MNRAS*, 379, 135
- Cardelli, J. A., Clayton, G. C., & Mathis, J. S. 1989, *ApJ*, 345, 245
- Charles, P. A., & Coe, M. J. 2006, *Compact stellar X-ray sources*, 215
- Chaty, S., et al. 2003, *MNRAS*, 346, 689
- Coppi, P. S. 1999, *High Energy Processes in Accreting Black Holes*, 161, 375
- Corbel, S., & Fender, R. P. 2002, *ApJL*, 573, L35
- Cunningham, C. 1976, *ApJ*, 208, 534
- Dagum, L. & Menon, R. 1998, *Computational Science & Engineering*, IEEE, 5, 46
- D'Angelo, C., Giannios, D., Dullemond, C., & Spruit, H. 2008, *A&A*, 488, 441
- De Villiers, J.-P., Hawley, J. F., Krolik, J. H., & Hirose, S. 2005, *ApJ*, 620, 878
- Di Salvo, T., Done, C., Życki, P. T., Burderi, L., & Robba, N. R. 2001, *ApJ*, 547, 1024
- Dubus, G., Lasota, J.-P., Hameury, J.-M., & Charles, P. 1999, *MNRAS*, 303, 139
- Dubus, G., Hameury, J.-M., & Lasota, J.-P. 2001, *A&A*, 373, 251
- Esin, A. A., McClintock, J. E., Drake, J. J., Garcia, M. R., Haswell, C. A., Hynes, R. I., & Muno, M. P. 2001, *ApJ*, 555, 483
- Falcke, H. 1996, *ApJL*, 464, L67
- Falcke, H., & Biermann, P. L. 1995, *A&A*, 293, 665
- Fender, R. 2006, *Compact stellar X-ray sources*, 381
- Fragile, P. C., & Meier, D. L. 2008, arXiv:0810.1082
- Frank, J., King, A., & Raine, D. J. 2002, *Accretion Power in Astrophysics*, by Juhan Frank and Andrew King and Derek Raine, Cambridge University Press.
- Frontera, F., et al. 2001, *ApJ*, 561, 1006
- Gallo, E., Migliari, S., Markoff, S., Tomsick, J. A., Bailyn, C. D., Berta, S., Fender, R., & Miller-Jones, J. C. A. 2007, *ApJ*, 670, 600
- Geist, A., Beguelin, A., Dongarra, J., Jiang, W., Manchek, R., & Sunderam, V. S. 1994, *Parallel Virtual Machine: A Users' Guide and Tutorial for Networked Parallel Computing*.
- Gelino, D. M., Balman, Ş., Kızıloğlu, Ü., Yılmaz, A., Kalemci, E., & Tomsick, J. A. 2006, *ApJ*, 642, 438
- Gierliński, M., Done, C., & Page, K. 2008, *MNRAS*, 388, 753
- Gierliński, M., Done, C., & Page, K. 2009, *MNRAS*, 392, 1106
- Gould, R. J., & Schröder, G. P. 1967, *Physical Review*, 155, 1404
- Greene, J., Bailyn, C. D., & Orosz, J. A. 2001, *ApJ*, 554, 1290
- Haardt, F., & Maraschi, L. 1993, *ApJ*, 413, 507
- Hannikainen, D., Campbell-Wilson, D., Hunstead, R., McIntyre, V., Lovell, J., Reynolds, J., Tzioumis, T., & Wu, K. 2001, *Astrophysics and Space Science Supplement*, 276, 45
- Hawley, J. F., Beckwith, K., & Krolik, J. H. 2007, *Ap&SS*, 311, 117
- Heavens, A. F., & Drury, L. O. 1988, *MNRAS*, 235, 997
- Henri, G., & Petrucci, P. O. 1997, *A&A*, 326, 87
- Hjellming, R. M., & Johnston, K. J. 1981, *ApJL*, 246, L141
- Hjellming, R. M., & Rupen, M. P. 1995, *Nature*, 375, 464
- Hjellming, R. M., et al. 2000, *ApJ*, 544, 977
- Homan, J., & Belloni, T. 2005, *Ap&SS*, 300, 107
- Homan, J., et al. 2005, *ApJ*, 624, 295
- Houck, J. C. 2002, *High Resolution X-ray Spectroscopy with XMM-Newton and Chandra*
- Hynes, R. I., Mauche, C. W., Haswell, C. A., Shrader, C. R., Cui, W., & Chaty, S. 2000, *ApJ*, 539, L37
- Hynes, R. I., Haswell, C. A., Chaty, S., Shrader, C. R., & Cui, W. 2002, *MNRAS*, 331, 169
- Hynes, R. I., Steeghs, D., Casares, J., Charles, P. A., & O'Brien, K. 2003, *ApJL*, 583, L95
- Hynes, R. I., Steeghs, D., Casares, J., Charles, P. A., & O'Brien, K. 2004, *ApJ*, 609, 317
- Hynes, R. I. 2005, *ApJ*, 623, 1026
- Hynes, R. I., et al. 2006, *ApJ*, 651, 401
- Jahoda, K., Markwardt, C. B., Radeva, Y., Rots, A. H., Stark, M. J., Swank, J. H., Strohmayer, T. E., & Zhang, W. 2006, *ApJS*, 163, 401
- Kardashev, N. S. 1962, *Soviet Astronomy*, 6, 317
- King, A. R., Kolb, U., & Burderi, L. 1996, *ApJL*, 464, L127
- King, A. R., Kolb, U., & Szuszkiewicz, E. 1997, *ApJ*, 488, 89
- Kondratko, P. T., Greenhill, L. J., & Moran, J. M. 2005, *ApJ*, 618, 618
- Lasota, J.-P. 2001, *New Astronomy Review*, 45, 449
- Levine, A. M., Bradt, H., Cui, W., Jernigan, J. G., Morgan, E. H., Remillard, R., Shirey, R. E., & Smith, D. A. 1996, *ApJL*, 469, L33
- McClintock, J. E., et al. 2001, *ApJ*, 555, 477
- McKinney, J. C., & Gammie, C. F. 2004, *ApJ*, 611, 977
- Maccarone, T. J. 2002, *MNRAS*, 336, 1371
- Magdziarz, P., & Zdziarski, A. A. 1995, *MNRAS*, 273, 837
- Maitra, D., & Bailyn, C. D. 2008, *ApJ*, 688, 537
- Markoff, S., Falcke, H., & Fender, R. 2001, *A&A*, 372, L25
- Markoff, S., Nowak, M., Corbel, S., Fender, R., & Falcke, H. 2003, *A&A*, 397, 645
- Markoff, S., Nowak, M. A., & Wilms, J. 2005, *ApJ*, 635, 1203
- Markoff, S., Bower, G. C., & Falcke, H. 2007, *MNRAS*, 379, 1519
- Markoff, S., et al. 2008, *ApJ*, 681, 905
- Meier, D. L. 2003, *New Astronomy Review*, 47, 667
- Meier, D. L. 2005, *Ap&SS*, 300, 55
- McClintock, J. E., Horne, K., & Remillard, R. A. 1995, *ApJ*, 442, 358
- McClintock, J. E., et al. 2001, *ApJ*, 551, L147
- McClintock, J. E., & Remillard, R. A. 2006, *Compact stellar X-ray sources*, 157
- Migliari, S., et al. 2007, *ApJ*, 670, 610
- Milgrom, M. 1978, *A&A*, 67, L25
- Miller, J. M., Ballantyne, D. R., Fabian, A. C., & Lewin, W. H. G. 2002, *MNRAS*, 335, 865
- Miller, J. M., Homan, J., & Miniutti, G. 2006, *ApJL*, 652, L113
- Miller, J. M., Homan, J., Steeghs, D., Rupen, M., Hunstead, R. W., Wijnands, R., Charles, P. A., & Fabian, A. C. 2006, *ApJ*, 653, 525
- Mitsuda, K., et al. 1984, *PASJ*, 36, 741
- Muñoz-Darias, T., Casares, J., & Martínez-Pais, I. G. 2008, *MNRAS*, 267
- Nakamura, M., & Meier, D. L. 2004, *ApJ*, 617, 123
- Narayan, R., Yi, I., & Mahadevan, R. 1995, *Nature*, 374, 623

- Narayan, R., Yi, I., & Mahadevan, R. 1996, *A&AS*, 120, 287
- Narayan, R., & McClintock, J. E. 2008, *New Astronomy Review*, 51, 733
- Noble, M. S., Houck, J. C., Davis, J. E., Young, A., & Nowak, M. 2006, *Astronomical Data Analysis Software and Systems XV*, 351, 481
- Nowak, M. A., Wilms, J., Heinz, S., Pooley, G., Pottschmidt, K., & Corbel, S. 2005, *ApJ*, 626, 1006
- Ogilvie, G. I., & Dubus, G. 2001, *MNRAS*, 320, 485
- Orosz, J. A., et al. 2001, *ApJ*, 555, 489
- Orosz, J. A., et al. 2002, *ApJ*, 568, 845
- Poutanen, J. 1998, *Theory of Black Hole Accretion Disks*, 100
- Ramadevi, M. C., & Seetha, S. 2007, *MNRAS*, 378, 182
- Rees, M. J. 1982, *The Galactic Center*, 83, 166
- Reis, R. C., Miller, J. M., & Fabian, A. C. 2009, *MNRAS*, in press (arXiv:0902.2793)
- Rieke, G. H., & Lebofsky, M. J. 1985, *ApJ*, 288, 618
- Rothschild, R. E., et al. 1998, *ApJ*, 496, 538
- Russell, D. M., Fender, R. P., Hynes, R. I., Brocksopp, C., Homan, J., Jonker, P. G., & Buxton, M. M. 2006, *MNRAS*, 371, 1334
- Russell, D. M., Maitra, D., Fender, R. P., & Lewis, F. 2008, in *VII Microquasar Workshop: Microquasars and Beyond* (arXiv:0811.2919)
- Rykoff, E. S., Miller, J. M., Steeghs, D., & Torres, M. A. P. 2007, *ApJ*, 666, 1129
- Shakura, N. I., & Sunyaev, R. A. 1973, *A&A*, 24, 337
- Shapiro, S. L., Lightman, A. P., & Eardley, D. M. 1976, *ApJ*, 204, 187
- Shimura, T., & Takahara, F. 1995, *ApJ*, 445, 780
- Stern, B. E., Begelman, M. C., Sikora, M., & Svensson, R. 1995, *MNRAS*, 272, 291
- Svensson, R. 1982, *ApJ*, 258, 321
- Svensson, R. 1986, , *IAU Colloq. 89: Radiation Hydrodynamics in Stars and Compact Objects*, 255, 325
- Yuan, F., Cui, W., & Narayan, R. 2005, *ApJ*, 620, 905
- van Paradijs, J., & McClintock, J. E. 1994, *A&A*, 290, 133
- Vrtilek, S. D., Raymond, J. C., Garcia, M. R., Verbunt, F., Hasinger, G., & Kurster, M. 1990, *A&A*, 235, 162
- Wilms, J., Nowak, M. A., Pottschmidt, K., Pooley, G. G., & Fritz, S. 2006, *A&A*, 447, 245
- Zimmerman, E. R., Narayan, R., McClintock, J. E., & Miller, J. M. 2005, *ApJ*, 618, 832
- Zurita, C., et al. 2002, *MNRAS*, 333, 791
- Zurita, C., et al. 2006, *ApJ*, 644, 432